J Biomol NMR (2013) 57:21–26
DOI 10.1007/s10858-013-9760-8

ARTICLE

Paramagnetic properties of the low- and high-spin states of yeast cytochrome *c* peroxidase

Sophie Vanwetswinkel · Nico A. J. van Nuland · Alexander N. Volkov

Received: 29 May 2013 / Accepted: 26 June 2013 / Published online: 6 July 2013

Abstract Here we describe paramagnetic NMR analysis of the low- and high-spin forms of yeast cytochrome *c* peroxidase (CcP), a 34 kDa heme enzyme involved in hydroperoxide reduction in mitochondria. Starting from the assigned NMR spectra of a low-spin CN-bound CcP and using a strategy based on paramagnetic pseudocontact shifts, we have obtained backbone resonance assignments for the diamagnetic, iron-free protein and the high-spin, resting-state enzyme. The derived chemical shifts were further used to determine low- and high-spin magnetic susceptibility tensors and the zero-field splitting constant (D) for the high-spin CcP. The D value indicates that the latter contains a hexacoordinate heme species with a weak field ligand, such as water, in the axial position. Being one of the very few high-spin heme proteins analyzed in this fashion, the resting state CcP expands our knowledge of the heme coordination chemistry in biological systems.

Keywords Paramagnetic NMR · Heme proteins · Pseudocontact shifts · Zero-field splitting

Electronic supplementary material The online version of this article (doi:10.1007/s10858-013-9760-8) contains supplementary material, which is available to authorized users.

S. Vanwetswinkel · N. A. J. van Nuland · A. N. Volkov (✉)
Jean Jeener NMR Centre, Structural Biology Brussels, Vrije Universiteit Brussel, Pleinlaan 2, 1050 Brussels, Belgium
e-mail: ovolkov@vub.ac.be

S. Vanwetswinkel · N. A. J. van Nuland · A. N. Volkov
Department of Structural Biology, VIB, Pleinlaan 2, 1050 Brussels, Belgium

Introduction

A large number of proteins contain native metal ions with unpaired electrons. These give rise to paramagnetic effects—in particular, paramagnetic relaxation enhancement (PRE) and hyperfine shifts—which can be detected by NMR spectroscopy and provide a rich seam of information on electronic and structural properties of metalloproteins (Arnesano et al. 2005; Ubbink et al. 2002). Manifested by the peak broadening in the NMR spectrum, PRE is an isotropic, r^{-6} distance-dependent effect, dictated by the electronic relaxation time of the metal centre (τ_s) and the rotational correlation time of the protein (τ_r). Hyperfine shifts include the Fermi (or contact) term—arising from delocalization of the spin density from the metal onto the ligand orbitals, which is negligible for the atoms few bonds away from the metal centre—and a dipolar (or pseudocontact) contribution. In contrast to the PREs, pseudocontact shifts (PCSs) are anisotropic, with the anisotropy determined by the spin state of the metal and the ligand field of its coordination sphere. The PCS is given by the Eq. (1):

$$\mathrm{PCS} = 1/(12\pi)r^{-3}\left[\Delta\chi_{ax}(3\cos^2\theta - 1) + 1.5\Delta\chi_{rh}\sin^2\theta\cos(2\varphi)\right] \quad (1)$$

where r, θ, and φ are the polar coordinates of the nuclear spin with respect to the principal axes of the magnetic susceptibility tensor (χ), and $\Delta\chi_{ax}$ and $\Delta\chi_{rh}$ are, respectively, the axial and rhombic $\Delta\chi$ components defined as $\Delta\chi_{ax} = \chi_{zz} - 0.5\ (\chi_{xx} + \chi_{yy})$ and $\Delta\chi_{rh} = \chi_{xx} - \chi_{yy}$, where χ_{xx}, χ_{yy}, and χ_{zz} are the principal components of the χ tensor (Ubbink et al. 2002). For the metalloproteins whose redox centres can exist in both paramagnetic and diamagnetic states, the PCSs can be determined from the differences in

the NMR chemical shifts of the protein in the two forms, $PCS = \delta_{para} - \delta_{dia}$, providing that no other factors (e.g. contact shifts, redox-dependent structural changes, discrepancies in the experimental conditions of the two samples) contribute to the measured chemical shift differences. This approach necessitates protein resonance assignment in both paramagnetic and diamagnetic forms.

Heme proteins have a long history of being studied by paramagnetic NMR (La Mar et al. 2000). Depending on the nature of the axial ligands, the heme Fe(III) ion can exist in low (S = 1/2), high (S = 5/2), and quantum-mixed (S = 1/2 + 3/2) spin states, all of which have distinct magnetic properties, which can be addressed by the PCS analysis. In the low-spin hemes, the $\Delta\chi$ anisotropy arises from the asymmetry of the electron g-tensor, while in the high-spin systems—with the ^{6}A ground state and an isotropic g-tensor—it is caused by the splitting of the energy levels in the absence of magnetic field (zero-field splitting, ZFS) (Walker 2000). Being a sensitive probe of the heme coordination environment (Walker and La Mar 1973), the ZFS constant, D, can be directly obtained from the $\Delta\chi_{ax}$ term derived from experimental PCSs, Eq. (2) (Tsan et al. 2001):

$$\Delta\chi_{ax} = -D\left[S(S+1)(2S-1)(2S+3)g^2\beta^2/(30k^2T^2)\right] \quad (2)$$

where S is the electron spin quantum number, g is the electron g-factor, β the Bohr magneton, k the Boltzmann constant, and T the temperature. In principle, this D determination strategy is suitable to a broad range of high-spin heme systems. However, in practice, its applicability has been thwarted by the scarcity of adequate diamagnetic references (reduced Fe(II) heme is often a paramagnetic, high-spin, S = 2 species), limited by large redox-dependent structural changes, and marred by the challenging assignment of the high-spin NMR spectra, suffering from large PREs. To the best of our knowledge, only two high-spin heme proteins—metaquomyoglobin (metMb-H_2O) (Kao and Lecomte 1993; Rajarathnam et al. 1991) and *Rhodobacter capsulatus* cytochrome *c*' (Cc') (Tsan et al. 2001)—were analyzed in this way.

Here we describe an extensive study by heteronuclear paramagnetic NMR spectroscopy of the low- and high-spin forms of yeast cytochrome *c* peroxidase (CcP), a 34.2 kDa enzyme involved in hydroperoxide reduction in mitochondria (Erman and Vitello 2002). The protein contains a *b*-type, non-covalently bound heme, ligated by a histidine residue and featuring a vacant coordination position available to small ligands. Depending on the enzyme preparation and the experimental conditions, CcP can exist in either 5- or 6-coordinate form (Bosshard et al. 1990). The present PCS analysis was made possible by the availability of a diamagnetic reference protein—the CcP harbouring the iron-free heme precursor protoporphyrin IX (CcP-PPIX)—and the fact that, along the polypeptide chain, the CcP-PPIX is isosteric with both the low-spin, cyanide-bound CcP (CcP-CN) and the high-spin, resting state enzyme (CcP-RS) (Bhaskar and Poulos 2005). Further, our inquiry was enabled by the extensive NMR resonance assignments of backbone atoms obtained in this work for all three CcP forms.

Results and discussion

CcP resonance assignment by conventional, triple-resonance NMR spectroscopy is a challenging task, which explains why previous studies were limited to several well-resolved protons of the heme and neighbouring residues (Banci et al. 1991; La Mar et al. 1995; Satterlee et al. 1983; Satterlee and Erman 1991). First, the large molecular weight of the system leads to fast transverse relaxation, resulting in broad resonances and decreased resolution in the NMR spectra. We partially solved this difficulty by the use of highly deuterated [^{2}H,^{13}C,^{15}N] CcP constructs (38 kDa) and transverse relaxation optimized spectroscopy (TROSY) NMR experiments, giving rise to an increased signal-to-noise ratio and improved spectral resolution (Volkov et al. 2013). Second, being a highly α-helical protein, CcP suffers from poor dispersion of the NMR chemical shifts. This problem is particularly acute for the CcP-PPIX, which is devoid of the iron atom that causes PCSs improving the resolution and, consequently, features crowded NMR spectra (Fig. S1). Third, the PREs experienced in the paramagnetic CcP forms lead to considerable signal broadening for the nuclei in the heme vicinity. Due to the slow electronic relaxation of the high-spin iron, the PREs are especially strong in the CcP-RS, with the protons located within 11 Å from the heme iron not observed in this work (Fig. 1). In an earlier report on the high-spin Cc', ^{1}H atoms as close as 9 Å from the iron could be resolved (Tsan et al. 2001), most likely due to higher signal-to-noise ratio afforded by concentrated protein samples (8 mM, compared to 1–1.5 mM employed here).

Providing that NMR assignments of a diamagnetic protein are known, PCSs can be used to assign backbone amide resonances in the paramagnetic form (Schmitz et al. 2006). Following this philosophy, we performed PCS-assisted backbone assignment of the CcP-PPIX and CcP-RS starting from the NMR spectra of the CcP-CN. The low-spin CcP-CN showed the optimal spectral quality—gaining from the PCS-caused boost in the spectral resolution and, at the same time, experiencing smaller PREs compared to the high-spin CcP-RS form—which enabled

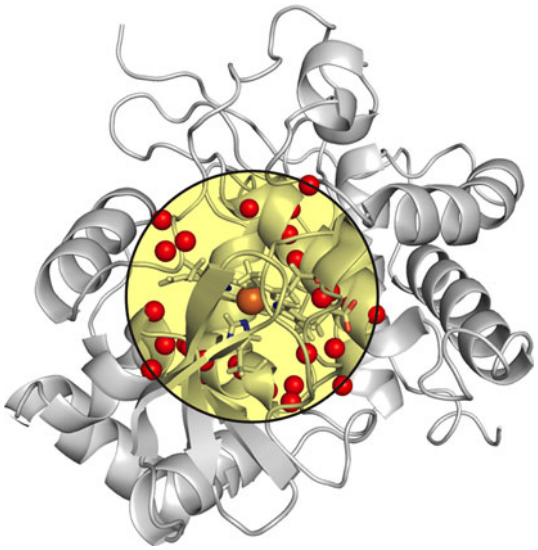

Fig. 1 The "blind spot" in the NMR resonance assignments of the high-spin CcP. The *highlighted* region shows HN atoms (*red spheres*) located within 11 Å from the heme iron (*orange sphere*). These protons are not observed in the NMR spectra of the CcP-RS due to large PREs caused by the high-spin (S = 5/2) Fe(III) atom. The heme group is shown in *sticks*

nearly-complete backbone resonance assignment by conventional three-dimensional (3D) NMR spectroscopy (Volkov et al. 2013). In the first step, using a series of NMR experiments, we assigned several-well resolved signals in the TROSY spectra of the CcP-PPIX, obtaining a set of 126 HN, C_α, C_β, and CO chemical shifts. These were used to calculate PCSs for the corresponding CcP-CN nuclei, which, in turn, were harnessed to determine the low-spin χ tensor (Equation 1). Knowing the χ tensor allows back-calculating the spectral positions of all CcP-PPIX resonances from their chemical shifts in the CcP-CN. This greatly simplifies the assignment procedure, which at this point mainly consists of verifying the identified resonances by establishing sequential connections in the 3D NMR experiments. Having assigned the CcP-PPIX spectra, the same strategy was extended to the CcP-RS, this time yielding PCSs and the χ tensor for the high-spin form, followed by the calculation of the CcP-RS peak positions from the CcP-PPIX chemical shifts and the final assignment verification. Alternatively, the CcP-RS peak positions were obtained directly from those of the CcP-CN, by calculating the *differences* in the PCSs, finding the solution for the *difference* between the low- and high-spin tensors—achieved by a grid-search of the 8 free parameters ($\Delta\chi_{ax}$, $\Delta\chi_{rh}$, θ, and φ for each tensor)—and back-calculating the spectral positions of the CcP-RS resonances. The two approaches yielded essentially the same results.

Having assigned the CcP-PPIX and CcP-RS NMR spectra (Figs. S1 and S2), a complete set of 793 (CcP-CN) or 568 (CcP-RS) PCSs for HN, C_α, C_β, and CO nuclei was determined and used to calculate the final low- and high-spin χ tensors (Fig. 2). In both cases, there is a good agreement between the observed and calculated PCSs (Figs. S3 and S4). Large violations are found only for several residues, located mostly in flexible loops or the regions disordered in the CcP-PPIX or CcP-RS X-ray structures (see Supporting Information for details). The close match between the observed and calculated PCSs suggests that the CcP crystallographic structure is retained in solution and there are no significant structural changes among the three CcP forms studied here. Indeed, discrepancies between PCS values can be used to track differences between the X-ray and solution structures of a given protein (Kao and Lecomte 1993) or highlight the regions undergoing redox-dependent structural changes (Volkov et al. 2012 and references therein).

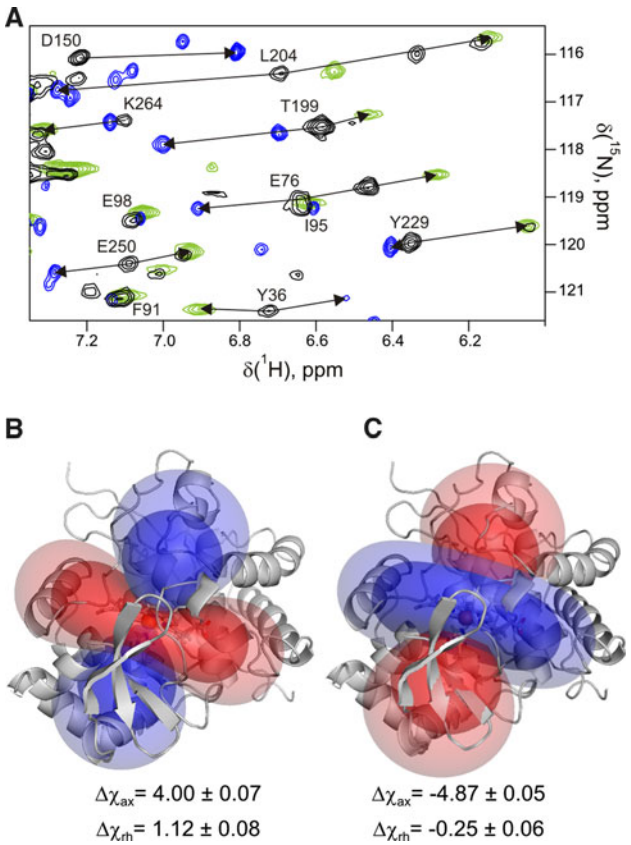

Fig. 2 Paramagnetic properties of the CcP in different spin-states. **a** A region of the overlaid [^{1}H, ^{15}N] TROSY spectra of the CcP-PPIX (*black*), CcP-CN (*blue*), and CcP-RS (*green*), with the arrows indicating PCSs of several backbone amides identified by the labels. Experimentally determined $\Delta\chi$ tensors of the **b** low-spin CcP-CN and **c** high-spin CcP-RS. The $\Delta\chi$ are in 10^{-32} m^3. The *blue* and *red* isosurfaces indicate positive and negative PCSs of ± 0.5 ppm (*dark shade*) and ± 0.2 ppm (*light shade*), respectively. The protein is in the same orientation as in Fig. 1

The CcP-CN χ tensor obtained in this work (Fig. 2b) is similar to those reported for other 6-coordinate, low-spin heme proteins, including cyanometmyoglobin (metMbCN) (Emerson and La Mar 1990), CN-bound horseradish peroxidase (HRP-CN) (La Mar et al. 1995) and eukaryotic cytochromes *c* (Volkov et al. 2012). In addition, it agrees well with that of the CcP-CN determined from a very limited dataset and based on the structural homology with metMbCN (La Mar et al. 1995). The long $\Delta\chi$ axis makes a 14° angle with the heme normal, in the same direction as the 10° tilt of the CN ligand in the CcP-CN X-ray structure (Edwards and Poulos 1990). This finding confirms earlier observations that the tilt of the axial ligand determines the direction of the major $\Delta\chi$ axis (La Mar et al. 2000).

The high-spin, CcP-RS χ tensor (Fig. 2c) displays very low rhombic anisotropy, exhibits sign inversion, and shows a decreased angle between the long $\Delta\chi$ axis and the heme normal (7°) with a concomitant change in the tilt direction as compared to the low-spin $\Delta\chi$ described above. The value of $\Delta\chi_{ax} = -4.87{\cdot}10^{-32}$ m^3 is strikingly similar to that of $-4.88{\cdot}10^{-32}$ m^3 reported for the high-spin Cc', which too showed nearly isotropic $\Delta\chi_{rh} \sim 0$ (Tsan et al. 2001). Calculating the ZFS constant from the CcP-RS $\Delta\chi_{ax}$ (Equation 2) yields D = 10.2 cm^{-1}, which can be compared to the reported values of 6.9 and 9.7 cm^{-1} for metMb-H_2O (Kao and Lecomte 1993; Rajarathnam et al. 1991) and 10.4 cm^{-1} for Cc' (Tsan et al. 2001), with the latter value matching closely the one determined in this work.

Early studies by La Mar and co-workers established that D could serve as a sensitive probe of the heme coordination, with weakening of the ligand field leading to higher D values (Rajarathnam et al. 1991; Walker and La Mar 1973). In particular, a large increase in D accompanying loss of the axial ligand can be used to reliably distinguish 5- from 6-coordinate heme groups (Rajarathnam et al. 1991). D values as large as 15.8 cm^{-1} were reported for the 5-coordinate high-spin heme in the *Aplysia* metmyoglobin (Rajarathnam et al. 1991).

The heme coordination status in the CcP-RS is a controversial subject. Depending on the enzyme preparation, storage, and the experimental conditions, the CcP-RS heme can exist as either 5- or 6-coordinate species or a mixture of both (Bosshard et al. 1990 and references therein). At pH 6.0, the freshly-prepared enzyme is predominantly 5-coordinate, while aged or frozen protein forms a hexacoordinate heme compound, with a weak field ligand such as water in the axial coordination position (Yonetani and Anni 1987). Being in a good agreement with the D = 9.7 cm^{-1} determined for the 6-coordinate metMb-H_2O (Kao and Lecomte 1993), the value of 10.2 cm^{-1} obtained in this work is indicative of a hexacoordinate heme species. Thus, it appears that in solution the CcP-RS iron has a fully occupied coordination sphere comprised of four porphyrin nitrogens, N_ε atom of H175 ligand, and a water molecule in the axial position.

Experimental section

Protein preparation

The uniformly-labeled, perdeuterated [^{2}H,^{13}C,^{15}N] CcP featuring a C-terminal (CcP-PPIX and CcP-CN) or N-terminal (CcP-RS) His-tag was prepared as described before (Volkov et al. 2013). The CcP-PPIX was obtained by the reconstitution of the apo protein with the protoporphyrin IX (Sigma), analogously to the hemin insertion (Volkov et al. 2013), except that the PPIX solution was made in 0.1 M NaOH and 15 % dimethyl sulfoxide (Bhaskar and Poulos 2005). The holo CcP concentrations were calculated from the UV–vis spectra using the extinction coefficients of $\varepsilon_{408} = 98.0$ (CcP-RS) (Yonetani and Anni 1987), $\varepsilon_{423} = 97.3$ (CcP-CN) (Volkov et al. 2013), and $\varepsilon_{408} = 96.0$ (CcP-PPIX) (Bhaskar and Poulos 2005) mM^{-1} cm^{-1}.

NMR spectroscopy

Backbone assignment experiments were conducted at 298 K on a four-channel Varian NMR Direct-Drive 800 MHz spectrometer equipped with a salt-tolerant PFG-Z cold probe. The samples contained 1–1.5 mM [^{2}H, ^{13}C, ^{15}N] CcP in 20 mM sodium phosphate 100 mM NaCl pH 6.0 and 6 % D_2O for the lock. The assignments were obtained from a series of TROSY-selected 2D [^{1}H,^{15}N] HSQC, 3D HNCO, deuterium-decoupled 3D HN(CA)CO, HNCA, HN(CO)CA, and out-and-back HN(CA)CB experiments as explained in the text. All NMR data were processed in NMRPipe (Delaglio et al. 1995) and analyzed in CCPN (Vranken et al. 2005). The resonance assignments determined in this work were deposited in the BMRB data bank under the accession numbers 19075 (CcP-PPIX) and 19076 (CcP-RS).

Paramagnetic NMR analysis and χ tensor calculations

In this work it is assumed that the unpaired electron is centered on the iron atom, while in fact it is distributed over the conjugated π-system of the heme. As this simplification holds only for the atoms 10 Å away from the metal center (Tsan et al. 2001), all atoms closer than that were excluded from the analysis. The 10 Å cut-off also eliminates the nuclei that experience contact shifts, leaving a set of atoms with pure PCS contribution. Being sensitive to small changes in the chemical environment and interactions with the neighboring atoms' orbitals (Boyd et al.

1999; Braun et al. 1994), N atoms show a high variance in the PCS correlation plots (Volkov et al. 2012) and, thus, were excluded from the present analysis.

The χ tensors were calculated with Numbat (Schmitz et al. 2008), starting from a set of measured PCS values (Tables S1 and S2) and using a high-resolution X-ray structure of the CcP-RS (PDB ID 1ZBY) (Bonagura et al. 2003). Atoms with $|PCS_{obs} - PCS_{calc}| > 0.2$ ppm were excluded from the initial dataset during iterative refinement of the χ tensors. The calculated tensors were corrected for the residual anisotropic chemical shifts (John et al. 2005), using the correction term implemented in Numbat (Schmitz et al. 2008). The errors on the $\Delta\chi$ parameters were estimated with the Numbat Monte-Carlo protocol (Schmitz et al. 2008) by adding 10 % of Gaussian noise to the atomic coordinates and experimental PCS values and randomly excluding 10 % of the working PCS dataset. The statistical variance—given by $\sigma^2 = \Sigma(PCS_{obs}\text{-}PCS_{calc})^2/(n\text{-}5)$, with the summation carried over all atoms (n) used in the fitting – was calculated for the final PCS datasets (bold in Tables S1-S2). For the low- and high-spin tensor determination, respectively, $\sigma^2 = 9{\cdot}10^{-3}$ (all atoms) and $4{\cdot}10^{-3}$ (atoms with $|PCS_{obs} - PCS_{calc}| > 0.2$ ppm excluded), and $\sigma^2 = 4{\cdot}10^{-3}$ (all atoms) and $3{\cdot}10^{-3}$ (atoms with $|PCS_{obs} - PCS_{calc}| > 0.2$ ppm excluded) were obtained. Several subsets of nuclei were used in the χ tensor calculations (Tables S1 and S2). Judging from the errors on the fitted parameters, the highest precision is achieved when an entire set of HN, C_α, C_β, and CO atoms is used as an input.

Acknowledgments A.N.V. is an FWO Post-Doctoral Researcher. We thank Yann Streckx for the critical reading of the manuscript. This work was supported by the VIB and the Flemish Hercules Foundation.

References

Arnesano F, Banci L, Piccioli M (2005) NMR structures of paramagnetic metalloproteins. Q Rev Biophys 38:167–219

Banci L, Bertini I, Turano P, Ferrer JC, Mauk AG (1991) Comparative ^{1}H NMR study of ferric low-spin cytochrome *c* peroxidase and horseradish peroxidase. Inorg Chem 30:4510–4516

Bhaskar B, Poulos TL (2005) The 1.13-Å structure of iron-free cytochrome *c* peroxidase. J Biol Inorg Chem 10:425–430

Bonagura CA, Bhaskar B, Shimizu H, Li H, Sundaramoorthy M, McRee DE, Goodin DB, Poulos TL (2003) High-resolution crystal structures and spectroscopy of native and compound I cytochrome *c* peroxidase. Biochemistry 42:5600–5608

Bosshard HR, Anni H, Yonetani T (1990) Yeast cytochrome *c* peroxidase. In: Everse J, Everse KE, Grisham MB (eds) Peroxidases in chemistry and biology. CRC Press, Boca Raton, pp 51–84

Boyd J, Dobson CM, Morar AS, Williams RJP, Pielak GJ (1999) ^{1}H and ^{15}N hyperfine shifts of cytochrome *c*. J Am Chem Soc 121:9247–9248

Braun D, Wider G, Wüthrich K (1994) Sequence-corrected ^{15}N "random coil" chemical shifts. J Am Chem Soc 116:8466–8469

Delaglio F, Grzesiek S, Vuister GW, Zhu G, Pfeifer J, Bax A (1995) NMRPipe: a multidimensional spectral processing system based on UNIX pipes. J Biomol NMR 6:277–293

Edwards SL, Poulos TL (1990) Ligand binding and structural perturbations in cytochrome *c* peroxidase. A crystallographic study. J Biol Chem 265:2588–2595

Emerson SD, La Mar GN (1990) NMR determination of the orientation of the magnetic susceptibility tensor in cyanometmyoglobin: a new probe of steric tilt of bound ligand. Biochemistry 13:1556–1566

Erman JE, Vitello LB (2002) Yeast cytochrome *c* peroxidase: mechanistic studies via protein engineering. Biochim Biophys Acta 1597:193–220

John M, Park AY, Pintacuda G, Dixon NE, Otting G (2005) Weak alignment of paramagnetic proteins warrants correction for residual CSA effects in measurements of pseudocontact shifts. J Am Chem Soc 127:17190–17191

Kao YH, Lecomte JTJ (1993) Determination of the zero-field splitting constant for proton NMR chemical shift analysis in metaquomyoglobin. The dipolar shift as a structural probe. J Am Chem Soc 115:9754–9762

La Mar GN, Chen Z, Vyas K, McPherson AD (1995) An interpretive basis of the hyperfine shifts in cyanide-inhibited horseradish peroxidase based on the magnetic axes and ligand tilt. Influence of substrate binding and extensions to other peroxidases. J Am Chem Soc 117:411–419

La Mar GN, Satterlee J, de Ropp JS (2000) Nuclear magnetic resonance of hemoproteins. In: Kadish KM, Smith KM, Guilard R (eds) The porphyrin handbook. Academic press, San Diego, pp 185–298

Rajarathnam K, La Mar GN, Chiu ML, Sligar SG, Singh JP, Smith KM (1991) ^{1}H NMR hyperfine shift pattern as a probe for ligation state in high-spin ferric hemoproteins: water binding in metmyoglobin mutants. J Am Chem Soc 113:7886–7892

Satterlee JD, Erman JE (1991) Proton NMR assignments of heme contacts and catalytically implicated amino-acids in cyanide-ligated cytochrome *c* peroxidase determined from one-dimensional and 2-dimensional nuclear Overhauser effects. Biochemistry 30:4398–4405

Satterlee JD, Erman JE, Lamar GN, Smith KM, Langry KC (1983) Assignment of hyperfine shifted resonances in high-spin forms of cytochrome *c* peroxidase by reconstitutions with deuterated hemins. Biochim Biophys Acta 743:246–255

Schmitz C, John M, Park AY, Dixon NE, Otting G, Pintacuda G, Huber T (2006) Efficient χ-tensor determination and NH assignment of paramagnetic proteins. J Biomol NMR 35:79–87

Schmitz C, Stanton-Cook MJ, Su X-C, Otting G, Huber T (2008) Numbat: an interactive software tool for fitting $\Delta\chi$-tensors to molecular coordinates using pseudocontact shifts. J Biomol NMR 41:179–189

Tsan P, Caffrey M, Daku ML, Cusanovich M, Marion D, Gans P (2001) Magnetic susceptibility tensor and heme contact shifts determination in the *Rhodobacter capsulatus* ferricytochrome *c*': NMR and magnetic susceptibility studies. J Am Chem Soc 123:2231–2242

Ubbink M, Worrall JAR, Canters GW, Groenen EJJ, Huber M (2002) Paramagnetic resonance of biological metal centers. Annu Rev Biophys Biomol Struct 31:393–422

Volkov AN, Vanwetswinkel S, Van de Water K, van Nuland NAJ (2012) Redox-dependent conformational changes in eukaryotic cytochromes revealed by paramagnetic NMR spectroscopy. J Biomol NMR 52:245–256

Volkov AN, Wohlkonig A, Soror SH, van Nuland NAJ (2013) Expression, purification, characterization, and solution nuclear magnetic resonance study of highly-deuterated yeast cytochrome *c* peroxidase with enhanced solubility. Biochemistry 52:2165–2175

Vranken WF, Boucher W, Stevens TJ, Fogh RH, Pajon A, Llinas M, Ulrich EL, Markley JL, Ionides J, Laue ED (2005) The CCPN data model for NMR spectroscopy: development of a software pipeline. Proteins 59:687–696

Walker FA (2000) Proton NMR and EPR spectroscopy of paramagnetic metalloporphyrins. In: Kadish KM, Smith KM, Guilard R (eds) The porphyrin handbook. Academic press, San Diego, pp 81–184

Walker FA, La Mar GN (1973) Nuclear magnetic resonance studies of ferric porphyrins. Ann N Y Acad Sci 206:328–348

Yonetani T, Anni H (1987) Yeast cytochrome c peroxidase. Coordination and spin states of heme prosthetic group. J Biol Chem 262:9547–9554